YALE PEABODY MUSEUM

JOURNAL OF MARINE RESEARCH

The *Journal of Marine Research,* one of the oldest journals in American marine science, published important peer-reviewed original research on a broad array of topics in physical, biological, and chemical oceanography vital to the academic oceanographic community in the long and rich tradition of the Sears Foundation for Marine Research at Yale University.

An archive of all issues from 1937 to 2021 (Volume 1–79) are available through EliScholar, a digital platform for scholarly publishing provided by Yale University Library at https://elischolar.library.yale.edu/.

Requests for permission to clear rights for use of this content should be directed to the authors, their estates, or other representatives. The *Journal of Marine Research* has no contact information beyond the affiliations listed in the published articles. We ask that you provide attribution to the *Journal of Marine Research.*

Yale University provides access to these materials for educational and research purposes only. Copyright or other proprietary rights to content contained in this document may be held by individuals or entities other than, or in addition to, Yale University. You are solely responsible for determining the ownership of the copyright, and for obtaining permission for your intended use. Yale University makes no warranty that your distribution, reproduction, or other use of these materials will not infringe the rights of third parties.

A generic length-scale equation for geophysical turbulence models

by L. Umlauf[1] and H. Burchard[2]

ABSTRACT

A generalization of a class of differential length-scale equations typically used in second-order turbulence models for oceanic flows is suggested. Commonly used models, like the k-ϵ model and the Mellor-Yamada model, can be recovered as special cases of this generic model, and thus can be rationally compared. In addition, a method is proposed that yields a generalized framework for the calibration of the most frequently used class of differential length-scale equations. The generic model, calibrated with this method, exhibits a greater range of applicability than any of the traditional models. Stratified flows, plane mixing layers, and turbulence introduced by breaking surface waves are considered besides some classical test cases.

1. Introduction

Together with the first attempts to apply so-called Reynolds-stress models to oceanographic problems almost three decades ago, an ongoing debate about the best choice for the equation determining the outer length-scale of turbulence in these models started. Numerous variables have been suggested since then, among the most successful ones the product of the turbulent kinetic energy, k, and the length scale of turbulence, l, in the model of Mellor and Yamada (1982) ('MY82' in the following), and the rate of dissipation, ϵ, in the k-ϵ model of Rodi (1987), 'R87'. Very recently, Umlauf *et al.* (2003) extended the k-ω model[3] of Wilcox (1988), 'W88', to buoyancy affected flows and compared with the MY82 and R87 models in typical oceanic situations.

Facing the fact that this list is far from complete, the problem of a rational and comprehensive evaluation of this class of models is evident. Various arguments have been used in the past to defend one or the other of these models. MY82 stated for example that an equation for ϵ is 'fundamentally wrong,' since a small-scale parameter like ϵ cannot describe a macro-scale of turbulence. R87 found this line of argumentation 'rather academic,' because equations for the length-scale determining variable are found most often in a quite empirical way.

1. Laboratoire d'Hydraulique Environnementale (LHE), Faculté ENAC, Ecole Polytechnique Féderalé de Lausanne, CH-1015 Lausanne, Switzerland. *email: lars.umlauf@epfl.ch*
2. Baltic Sea Research Institute, Seestrasse 15, D-18119 Rostock-Warnemunde, Germany.
3. ω is defined as the specific dissipation rate $\omega \propto \epsilon/k$.

In this context, it should be noted that virtually all Reynolds-stress and two-equation models adopt, explicitly or implicitly, the classical cascading model $\epsilon \propto k^{3/2} l^{-1}$. This relation, or its mathematical equivalent formulated in any other variable, can be used to express the transport equation for one variable (say, ϵ) in terms of any other (say, kl). Hence, *physically,* there is no objective advantage in formulating a transport equation for a particular variable instead of any other. *Mathematically* and *numerically,* however, the properties of the corresponding model can be strongly affected by the choice for the length-scale determining variable. An example is the inconvenient requirement of a wall-function in the kl equation of MY82 to reproduce the fundamental law of the wall. Neither the R87 nor the W88 model require such modifications. Due to very similar parameterisations, however, all three models can be considered as physically identical.

Even though there are a number of attempts to compare the properties of *existing* models for the length-scale equation (e.g. Speziale *et al.,* 1990; Wilcox, 1998; Burchard *et al.,* 1998; Burchard and Petersen, 1999; Umlauf *et al.,* 2003), we found no rational investigation of the interesting question about the optimal choice of the length-scale variable and its transport equation considering *all* possibilities among a given class of models. The generic transport equation for the turbulent length-scale presented here is a tool to evaluate this question. Besides this, all traditional models can be recovered as special cases of this generic equation, and hence can be conveniently compared. We derive a set of analytical solutions of this generic model, use them to calibrate the model constants, and demonstrate the fundamental properties of the whole class of models. In a general framework, we illustrate the sensitivity and fragility of these models with respect to parameter changes. Besides the analysis of the properties of this class of models, the main result is a reliable and robust length-scale equation with almost fully controlled properties and a greater range of applicability in marine modelling than any of the traditional models.

The outline of the paper is as follows. In Section 2, we suggest a general framework for the transport equation of the length-scale determining variable for the family of models discussed here. Together with the transport equation for k and a so-called Algebraic Reynolds-Stress Model (ASM), a generic two-equation model is defined. In Section 3, the model parameters of this generic model are restricted by applying it to some standard, in particular stratified, turbulent flows. In addition, the pure balance between turbulent transport and dissipation in shear-free, unstratified and stationary turbulence is considered in detail. It is demonstrated how this flow relates to some recently published models for the effects of breaking surface waves in the ocean. An analytical solution of the non-linear set of differential equations describing this flow is suggested and the performance of a number of well-known two-equation models in the wave-breaking case is investigated. It is demonstrated in Section 4 how the form of the generic length-scale can be restricted by combining all constraints and investigating their interrelations. We use Section 5 to confirm the analytical findings with some numerical results, present an oceanographic application, and finally draw our conclusions in Section 6.

2. The generic model

In this section, we present a transport equation for the generic length-scale ψ defined below. This equation generalizes the traditional transport equations used in marine modeling. It can either be solved in the context of any higher-order turbulence closure model, or it can be regarded as the second equation of a generic two-equation model. Then, it is solved simultaneously together with the classical transport equation for the turbulent kinetic energy, k.

We formulate the transport equation for ψ as simply as possible. Nevertheless, it is general enough to identify a number of well-known two-equation models used in oceanography and meteorology as special cases of the generic model for appropriate parameter sets. Thus, the concept outlined here allows for a rational and comprehensive investigation of these models. Among them are the k-ϵ model (in the form presented by R87), the k-ω model of W88 as modified by Umlauf *et al.* (2003), and the model of Zeierman and Wolfshtein (1986) ('ZW86' presently not used in geophysical modeling). Some two-equation models, however, do not entirely fit in the framework of the generic model and have to be treated separately. An example is the k-kl model of MY82. Because of its outstanding position in geophysical modeling, we shall discuss some aspects of this model explicitly.

a. The generic two-equation model

The first equation of the generic two-equation model introduced here describes the evolution of the turbulent kinetic energy, k. This quantity is balanced according to

$$\frac{\partial k}{\partial t} + u_i \frac{\partial k}{\partial x_i} = \mathcal{D}_k + P + G - \epsilon, \tag{1}$$

which follows immediately from the contraction of the transport equation of the Reynolds stress tensor, $\langle u_i' u_j' \rangle$. Here and in the following, u_i and u_i' refer to the components of the mean and fluctuating parts of the velocity vector in the direction of the Cartesian coordinates x_i, and $\langle \cdots \rangle$ denotes the ensemble average. $\mathcal{D}_k$ summarizes the turbulent and viscous transport terms, and ϵ is the rate of dissipation of k. P and G relate to the production of turbulent kinetic energy by mean shear and buoyancy.

The solution of (1) requires the knowledge of ϵ. In addition, common closure assumptions for the unknown correlation terms in the transport equations for the higher moments also require the prescription of a field uniquely determining the outer time-scale of turbulence, τ. This quantity may be calculated from k and the rate of dissipation, ϵ, but equally well from any of the other fields already mentioned.

Here, we suggest a generalization of the different approaches by formulating a transport equation for a 'generic' statistical field variable, ψ. We require that ψ is uniquely related to the fields of k and ϵ according to

$$\psi = \tilde{\psi}(k, \epsilon), \tag{2}$$

where $\tilde{\psi}$ denotes an invertible function. Then, ϵ can be computed for any given pair of k and ψ, and other turbulent quantities are easily obtained; e.g., the integral length-scale, l, can be derived from the spectral transport relation

$$l = (c_\mu^0)^3 \frac{k^{3/2}}{\epsilon},$$ (3)

where c_μ^0 denotes a constant of the model. We restrict the functional form of $\tilde{\psi}$ in (2) further by assuming that its dependence on k and ϵ can be separated by products of powers of these quantities,

$$\psi = (c_\mu^0)^{\bar{p}} k^{\bar{m}} \epsilon^{\bar{n}},$$ (4)

where the exponents $\bar{p}$, $\bar{m}$, $\bar{n}$ are real numbers, and the model constant appearing in (4) is expressed in terms of c_μ^0 for convenience. It is evident from (3) that this equation is identical to an equation of the form

$$\psi = (c_\mu^0)^p k^m l^n,$$ (5)

which we prefer here for reasons explained below.

Now, we formulate a transport equation for the variable ψ of the form

$$\frac{\partial \psi}{\partial t} + u_i \frac{\partial \psi}{\partial x_i} = \mathcal{D}_\psi + \frac{\psi}{k} (c_{\psi 1} P + c_{\psi 3} G - c_{\psi 2} \epsilon),$$ (6)

where $\mathcal{D}_\psi$ denotes the turbulent and viscous transport terms of ψ, and $c_{\psi 1}$, $c_{\psi 2}$, and $c_{\psi 3}$ are model constants. The shape of (6) is suggested by the traditional model equations for ϵ, kl, and ω used in ocean modelling. Additionally, (6) is the simplest, dimensionally correct form including the effects of turbulent transport, shear production, buoyancy production and dissipation. It would have been possible to add more terms to the right-hand side of (6) to account for some more aspects of rotation and stratification. For the introduction and investigation of the basic properties of the generic model, however, we considered it completely sufficient to use the simple form (6).

With ψ following from (6), the rate of dissipation, ϵ, can be computed from (5) and (3) according to

$$\epsilon = (c_\mu^0)^{3 + (p/n)} k^{(3/2) + (m/n)} \psi^{-(1/n)}.$$ (7)

For appropriate values of the exponents p, m, n in (5), a number of well-known models can be directly recovered from (6). Some examples are given in Table 1. Model constants for these models are compiled in Table 2.

It should be noted here that the factor $(c_\mu^0)^p$ appearing in (5) has been introduced only to make ψ completely identifiable with any of the traditional variables like kl, ϵ, and ω by simply adopting the parameters from Table 1. Mathematically, however, this factor is

Table 1. Exponents p, n, m defined in (5) and relation to the variable of the second equation in some well-known two-equation models.

ψ	Two-equation model by:	p	m	n
ω	Wilcox (1988)	-1	$\frac{1}{2}$	-1
kl	Mellor and Yamada (1982)	0	1	1
ϵ	Rodi (1987)	3	$\frac{3}{2}$	-1
$k\tau$	Zeierman and Wolfshtein (1986)	-3	$\frac{1}{2}$	1

irrelevant. This is easily understood from the fact that (6) (with $\mathcal{D}_\psi$ modelled according to (11) below) can be multiplied by *any* constant without changing the solution.

We want to point out that not all models fit perfectly well in the framework of the transport equation (6). The model of MY82 e.g. requires so-called wall functions to correctly reproduce the logarithmic part of the law of the wall and also differs slightly in the formulation of the turbulent transport terms. Strictly speaking, for this model the values of the Schmidt-numbers in Table 2 apply only in the logarithmic wall layer (see Mellor and Yamada, 1982).

b. The generic model in horizontally homogeneous flows

In horizontally homogeneous flows, in which mean and turbulent quantities (except the mean pressure) are assumed to vary only in the direction of the vertical coordinate, z, aligned with the acceleration of gravity, g, the fundamental properties of the generic model can be investigated with purely analytical tools. Horizontally homogeneous flows are also a useful first order approximation for many geophysical situations. For these reasons, we restrict ourselves to such flows in the following.

With the above assumptions, the shear and the buoyancy production, P and G, can be expressed according to[4]

$$P = -\langle u'w'\rangle \frac{\partial u}{\partial z} - \langle v'w'\rangle \frac{\partial v}{\partial z} = v_t M^2, \qquad G = g\alpha\langle\theta'w'\rangle = -v_t^\theta N^2, \qquad (8)$$

where θ denotes the temperature and α the volumetric expansion coefficient[5]. v_t and v_t^θ are the vertical turbulent diffusivities of momentum and heat, and

$$M^2 = \left(\frac{\partial u}{\partial z}\right)^2 + \left(\frac{\partial v}{\partial z}\right)^2, \qquad N^2 = g\alpha\frac{\partial\theta}{\partial z} \qquad (9)$$

are referred to as the (squares of the) shear frequency and the buoyancy frequency, respectively.

---

4. We use $u = u_1$, $v = u_2$, $w = u_3$ and $x = x_1$, $y = x_2$ and $z = x_3$.
5. For simplicity, it is assumed here that buoyancy is only due to thermal expansion.

Table 2. Model constants of some standard models converted to the notation used here. The values of $c_{\psi 3}$ for the models of W88 and R87 are discussed in Section 3d.

	c_μ^0	σ_k^ψ	σ_ψ	$c_{\psi 1}$	$c_{\psi 2}$	$c_{\psi 3}$
k-ω (W88):	0.5477	2	2	0.555	0.833	(see text)
k-kl (MY82):	0.5544	1.96	1.96	0.9	0.5	0.9
k-ϵ (R87):	0.5477	1.0	1.3	1.44	1.92	(see text)
k-τ (ZW86):	0.5477	1.46	10.8	0.173	0.225	(—)

With the Algebraic Stress Models (ASMs) typically used in geophysical turbulence models, the vertical turbulent diffusivities in horizontally homogeneous flows can be expressed as

$$\nu_t = c_\mu k^{1/2} l, \qquad \nu_t^\theta = c_\mu' k^{1/2} l, \tag{10}$$

where c_μ and c_μ' are sometimes referred to as the 'stability functions.'[6] The stability functions follow directly without further assumptions from the ASM and depend non-linearly on nondimensional parameters describing the stability of the flow, such as the shear-number, $S = k/\epsilon |M|$, or the turbulent Froude-number, $Fr = Nl/k^{1/2}$ (Mellor and Yamada, 1974; Canuto *et al.*, 2001). Note that $c_\mu = c_\mu^0$ in the unstratified logarithmic boundary layer by definition. The particularly simple forms of (8) and (10) in horizontally homogeneous flows allow for simple analytical solutions of the model equations retaining, however, the complete information of the ASM. An extensive amount of literature is available about stability functions and their derivation, and hence this topic will be addressed only very briefly below (see e.g. Burchard and Bolding (2001) and the references therein).

For compatibility with the traditional models, the turbulent transport terms $\mathscr{D}_k$ and $\mathscr{D}_\psi$, appearing in (1) and (6) are expressed by gradient formulations,

$$\mathscr{D}_k = \frac{\partial}{\partial z}\left(\nu_k^\psi \frac{\partial k}{\partial z}\right), \qquad \mathscr{D}_\psi = \frac{\partial}{\partial z}\left(\nu_\psi \frac{\partial \psi}{\partial z}\right), \tag{11}$$

where the diffusivities of k and ψ are related to the eddy diffusivity, ν_t, according to

$$\nu_k^\psi = \frac{\nu_t}{\sigma_k^\psi}, \qquad \nu_\psi = \frac{\nu_t}{\sigma_\psi} \tag{12}$$

via the constant Schmidt-numbers, σ_k^ψ and σ_ψ.

---

6. Note, that the function c_μ defined here is different from a constant of the same name used by R87 for the standard k-ϵ model.

3. Constraints on the model parameters

Any second-order model is expected to yield reasonable results in some standard situations like the decay of homogeneous turbulence behind a grid or the logarithmic region of the law of the wall. Usually, reliable measurements exist in such situations and it is straightforward to adjust the model parameters accordingly and hope that the model will yield reliable extrapolations also to non-standard situations.

In this section, we investigate the properties of the generic model (1) and (6) in some fundamental flows commensurate with the approximations introduced in Section 2b. These flows, though being fundamental, are evidently also highly relevant in marine modelling. More specific oceanographic flows are considered below.

If it is assumed that the application of the model to each standard flow results in a constraint on the model parameters in form of an algebraic equation independent of all others, the number of constraints that can be satisfied at most is identical to the number of model parameters. In the case of the traditional models, these are the six parameters are c_μ^0, $c_{\psi 1}$, $c_{\psi 2}$, $c_{\psi 3}$, σ_k^ψ, and σ_ψ. Hence, with any model of this type it will be impossible to account for more than six *independent* constraints. However, if the structure of the model itself (i.e. the power exponents m and n appearing in (5)) is considered variable, two new degrees of freedom can be gained. We shall refer to this property of the generic model as its *polymorphism* in the following. Clearly, there may as well exist a number of constraints that are *not* independent and hence cannot be satisfied by simply calibrating model parameters. In such cases, the quality of the model determines, whether such constraints can be satisfied, at least approximately, or not. An example will be encountered in Section 3c.

a. The logarithmic boundary layer

The first constraint follows from an application of the generic model to the logarithmic boundary layer near rigid surfaces. If we define the friction velocity, $u_* = (\tau_w/\rho)^{1/2}$ (τ_w is the shear-stress at the wall), the von Kármán constant, κ, and the distance from a rigid wall, z, well-known relations like $l = \kappa z$ and $\partial u/\partial z = u_*/(\kappa z)$ can be shown to hold[7]. With the help of the transport equation of the turbulent kinetic energy, (1), it can be demonstrated that the generic model predicts a constant k throughout the logarithmic layer according to

$$k = \frac{u_*^2}{(c_\mu^0)^2}. \tag{13}$$

The constant $(c_\mu^0)^2$ is known to adopt a value of $(c_\mu^0)^2 \approx 0.3$ (see Townsend, 1976; Mellor and Yamada, 1982). It is a basic requirement for any stability function, c_μ, defined in (10), to converge to this value in the logarithmic boundary layer.

---

7. It is assumed that the turbulent scale, l, introduced in (3) coincides with Prandtl's mixing length, κz, close to walls.

Table 3. Model parameters consistent with (14). The values have been derived by assuming the standard value $c_\mu^0 = 0.5477$ for the k-ω model, the k-ϵ model and the k-$k\tau$ model, and $c_\mu^0 = 0.5544$ for the MY82 model. Note, that the MY82 model requires an additional wall-function to yield $\kappa = 0.4$.

	k-ω (W88)	k-kl (MY82)	k-ϵ (R87)	k-$k\tau$ (ZW86)
κ (orig.):	0.409	0.4	0.433	0.41
$\kappa = 0.4$:	$\sigma_\omega = 1.92$	$\sigma_l = 1.96$	$\sigma_\epsilon = 1.11$	$\sigma_\tau = 10.26$

The second constraint arises from the insertion of the law-of-the-wall relations in the second equation of the generic model, (6). To be compatible with the law of the wall, this equation requires that

$$\sigma_\psi = \frac{n^2\kappa^2}{(c_\mu^0)^2(c_{\psi 2} - c_{\psi 1})}. \tag{14}$$

With the exponent n taken from Table 1, corresponding relations for the traditional two-equation models can be easily constructed from this equation.

Table 3 summarizes some model constants satisfying the compatibility relation (14). The MY82 model computes a value of $\kappa = 0.4$ only when a term resulting from the wall function of this model is added to $c_{\psi 2}$ in (14) (see Umlauf *et al.*, 2003). Note the high value of the standard R87 model.

b. *Decay of homogeneous turbulence*

Another example of a simple but fundamental turbulent situation is the temporal decay of isotropic, homogeneous turbulence (approximated by the spatial decay of turbulence behind grids in laboratory settings). At large times, t, data from many experiments are well described by a power law of the form

$$\frac{k}{k_0} = A\left(\frac{t}{\tau_0}\right)^d, \tag{15}$$

with constant A and initial values of the kinetic energy, k_0, and the *eddy turnover time, τ_0*. The decay rates, d, have been thoroughly documented. Experiments (Bradshaw, 1975; Townsend, 1976; Domaradzki and Mellor, 1984; Mohamed and Larue, 1990) suggest that d is in the range $-1.3 < d < -1$. DNS, generally conducted at low Reynolds numbers, produce consistently higher values. For example, Briggs *et al.* (1996) obtain a value near -1.5 from their DNS. Here, we adopt the intermediate value $d = -1.2$ and remark that none of results presented below is sensitive with respect to small changes in d.

In homogeneous decaying turbulence, (1) and (6) reduce to a balance between the rate and dissipation terms, respectively. The coupled system of ordinary differential equations can be solved for given initial values k_0 and ψ_0. The solution can be shown to reduce to (15) at large times. Then, the decay exponent, d, is determined by

Table 4. Temporal decay rate, d, for homogeneous, unstratified turbulence as computed by different two-equation models.

	k-ω (W88)	k-kl (MY82)	k-ϵ (R87)	k-$k\tau$ (ZW86)
decay rate d	-1.2	-1	-1.087	-1.29

$$d = -\frac{2n}{2m + n - 2c_{\psi 2}}, \tag{16}$$

and thus depends only on the structure of the model (i.e. m and n) and the model constant $c_{\psi 2}$. For given exponents m and n, the experimental value of d implies the third fundamental constraint on the model parameters. Note, that the predicted decay rate, d, is completely independent of the ASM.

The decay rates for k predicted by some models[8] are summarized in Table 4. It can be seen that all models compute results in the range of the measurements, and, in fact, most models have been calibrated to perform well in this situation.

c. Homogeneous turbulent shear flow

A natural extension of decaying homogeneous turbulence is the inclusion of an homogeneous shear and an aligned homogeneous stratification. Since turbulence is still assumed to be homogeneous, the divergence of any turbulent transport term vanishes and the intricate interplay between the stabilizing effects of stratification and the destabilizing action of shear can be isolated. Thus, it is not surprising that this highly interesting special case of turbulence has been explored extensively by laboratory experiments (Tavoularis and Corrsin, 1981a,b; Tavoularis and Karnik, 1989; Rohr *et al.*, 1988), by Direct Numerical Simulation (Gerz *et al.*, 1989; Holt *et al.*, 1991; Jacobitz *et al.*, 1997; Shih *et al.*, 2000) and by Large-Eddy Simulation (Kaltenbach *et al.*, 1994). That flows of this kind are also crucial in many oceanographic flows has recently been pointed out by Baumert and Peters (2000).

In the context of the generic two-equation model, this turbulent flow is mathematically established by neglecting the turbulent transport terms and the advective part of the material time derivative. Then, (1) and (6) reduce to a set of ordinary differential equations and it can be shown that all two-equation models discussed here are isomorphic (Baumert and Peters, 2000).

Using the chain rule of differentiation, the relation

$$\frac{1}{l}\frac{dl}{dt} = \frac{1}{n}\frac{1}{\psi}\frac{d\psi}{dt} - \frac{m}{n}\frac{1}{k}\frac{dk}{dt} \tag{17}$$

---

8. (16) also applies to the MY82 model, since homogeneous turbulence can only occur distant from walls, where the influence of the wall function of this model is negligible.

for the mixing length, l, follows immediately from (5). With (17), the generic model expressed by (1) and (6) can be used to derive an evolution equation for the integral length scale, l,

$$\frac{1}{l}\frac{dl}{dt} = -\left(\frac{1}{n}c_{\psi_2} - \frac{m}{n}\right)\frac{\epsilon}{k} + \frac{1}{k}\left(\left(\frac{1}{n}c_{\psi_1} - \frac{m}{n}\right)P + \left(\frac{1}{n}c_{\psi_3} - \frac{m}{n}\right)G\right). \tag{18}$$

Completely analogous, the turbulent time-scale, $\tau = k/\epsilon$, evolves according to

$$\frac{1}{\tau}\frac{d\tau}{dt} = -\left(\frac{1}{n}c_{\psi_2} - \frac{m}{n} - \frac{1}{2}\right)\frac{\epsilon}{k} + \frac{1}{k}\left(\left(\frac{1}{n}c_{\psi_1} - \frac{m}{n} - \frac{1}{2}\right)P + \left(\frac{1}{n}c_{\psi_3} - \frac{m}{n} - \frac{1}{2}\right)G\right). \tag{19}$$

Tennekes (1989) derived an equation similar to (18) (however only for the special case of the k-ϵ model applied to unstratified flows) and stated that '*on dimensional grounds, l cannot depend upon the shear because the shear is homogeneous and cannot impose a length scale*' (also see Baumert and Peters (2000)). Since the shear production, P, of course, depends on the shear, this important statement requires the factor in front of P in (18) to vanish[9]. This leads to the fourth fundamental constraint,

$$c_{\psi 1} = m. \tag{20}$$

Comparison of the values of m from Table 1 with the actual model parameter $c_{\psi 1}$ from Table 2 illustrates that, in fact, all models, except the model of ZW86, are close to this constraint. The value $c_{\epsilon 1} = 3/2$, given in Table 1 for the k-ϵ model, corresponds precisely to the value suggested by Tennekes (1989) for this model.

There is considerable experimental support for the theoretical argument of Tennekes. Tavoularis and Karnik (1989) compiled a large number of laboratory results of quasi-homogeneous turbulence subject to a homogeneous shear (but without active stratification) and explicitly stated that the growth rate of the integral scale 'is essentially independent of the shear.' Besides this, many experiments and numerical investigations cited in the introduction to this subsection indicate that for situations with strong shear, turbulence reaches a state of 'structural equilibrium,' in which the turbulent time-scale, τ, is approximately constant and the turbulent parameters exhibit exponential growth[10]. It is easy to show that for $\dot{\tau} = 0$ also the generic model predicts exponential growth of turbulent quantities like k or the Reynolds stress tensor, $\langle u_i' u_j' \rangle$.

It is instructive to look at the implications of Tennekes argument for unstratified flows in structural equilibrium in the context of the generic model. First, it should be noted that in structural equilibrium the left hand side of (19) is zero by definition (τ is constant). Then, (19) becomes algebraic and can easily be solved for $c_{\psi 1}$, yielding

---

9. Evidently, the same argument does not apply to the buoyancy term in (18). It is well-known that buoyancy does set an upper limit (usually referred to as the Ozmidov-scale) to the vertical turbulent length-scale also in homogeneous turbulence.

10. This statement applies at least to the high Reynolds-number runs in the recent DNS of Shih *et al.* (2000).

$$c_{\psi 1} = m + n\left(\frac{\epsilon}{P}\left(\frac{1}{n}\,c_{\psi 2} - \frac{m}{n} - \frac{1}{2}\right) + \frac{1}{2}\right), \tag{21}$$

or, by expressing $c_{\psi 2}$ with the help of (16),

$$c_{\psi 1} = m + n\left(\frac{\epsilon}{P}\frac{1}{d} + \frac{1}{2}\right). \tag{22}$$

Comparison with (20) reveals that models calibrated according to Tennekes argument, and according to (16), in structural equilibrium necessarily require

$$\frac{\epsilon}{P} = -\frac{d}{2}, \tag{23}$$

completely independent of the ASM. For a commonly accepted value of $d = -1.2$ (see above), one obtains $\epsilon/P = 0.6$, not far from $\epsilon/P \approx 0.68$, suggested by Tavoularis and Karnik (1989). Above this, expressing the shear-production, P, according to (8) and using (3) and (10), it is a few algebraic steps to show that

$$\frac{\epsilon}{P} = \frac{1}{c_{\mu}^{\epsilon}S^2} = -\frac{d}{2}, \tag{24}$$

where we used

$$c_{\mu}^{\epsilon} = (c_{\mu}^0)^3 c_{\mu}, \qquad S = \frac{k}{\epsilon}|M| \tag{25}$$

for convenience.

Since the stability function c_{μ}^{ϵ}, resulting from an appropriate ASM, in general depends on the shear number, S, the second equality in (24) constitutes a non-linear equation for S. As an example, we discuss a stability function recently suggested by Canuto *et al.* (2001), which simplifies in the absence of stratification according to

$$c_{\mu}^{\epsilon} = \frac{0.107 - 0.00012S^2}{1 + 0.0287S^2 - 0.0000337S^4}, \tag{26}$$

(see Burchard and Bolding, 2001). Solving (24) for this stability function, a shear-number of $S = 5.39$ is computed, close to the value $S \approx 5$ suggested by many laboratory experiments (see Wilcox, 1998). Note, that the stability function of Canuto *et al.* (2001) adopts the value $c_{\mu}^{\epsilon} = 0.057$ in structural equilibrium, considerably lower than the value $c_{\mu}^{\epsilon} = 0.09$ used in the standard models of ZW86, R87, and W88. The predicted dimensionless shear-stress $\langle u'w'\rangle/k = -0.31$ is in good agreement with the value $\langle u'w'\rangle/k \approx -0.32$ found by Tavoularis and Karnik (1989). Thus, Tennekes argument leads to a highly consistent behaviour of the generic model in structural equilibrium and hence (20) proves to be a simple but powerful constraint.

Another interesting result can be obtained from the combination of some of the previous

findings. Expressing $c_{\psi 2}$ and $c_{\psi 1}$ by (16) and (20), respectively, the compatibility relation (14) can be re-written as

$$\sigma_\psi = \frac{2\kappa^2 d}{(c_\mu^0)^2 (d + 2)} \, n,$$ (27)

which illustrates that for all meaningful values of the temporal decay rate, $-2 < d < 0$, the exponent of the length-scale, n, must be negative in order to insure $\sigma_\psi > 0$. Thus, all models with positive n will require additional wall-functions. This is in particular true for the k-kl model of MY82 with $n = 1$.

d. Mixed layer deepening

The correct prediction of mixed layer deepening into a stratified fluid due to a wind stress at the surface is one of the most crucial requirements for an oceanic turbulence model. This situation has been frequently interpreted by analogy with the classical experiment of Kato and Phillips (1969) and its re-interpretation by Price (1979), in which the entrainment in a linearly stratified fluid subject to a constant surface stress was investigated. The results of this experiment have been used by numerous authors to calibrate their turbulence models.

In particular, it has been shown by Burchard and Bolding (2001) for the R87 model, by Burchard (2001a) for the MY82 model, and by Umlauf *et al.* (2003) for the W88 model that, remarkably, the mixed layer depth predicted by these models depends almost exclusively on the value of the Richardson number, $Ri = N^2/M^2$, computed in a *homogeneous,* stratified shear-flow in steady-state. This value is usually referred to as the steady-state Richardson number, Ri_{st} (Rohr *et al.,* 1988; Kaltenbach *et al.,* 1994; Jacobitz *et al.,* 1997; Shih *et al.,* 2000).

Generalizing the procedure of the above authors, we first assume $\dot{\tau} = 0$ and $P + G = \epsilon$ in (19). Then, expressing the production terms P and G by (8) and (10), the steady-state Richardson number, Ri_{st}, follows from (19) according to

$$Ri_{st} = \frac{c_\mu}{c_\mu'} \frac{c_{\psi 2} - c_{\psi 1}}{c_{\psi 2} - c_{\psi 3}}.$$ (28)

Since it is well-known that, with the equilibrium assumption, stability functions reduce to functions of Ri only (Mellor and Yamada, 1974; Galperin *et al.,* 1988), (28) is a nonlinear equation for the model constant $c_{\psi 3}$ for given Ri_{st}. Note, that the structure parameters, m and n, do not appear in (28). This implies that the type of the two-equation model is irrelevant for the prediction of the mixed layer depth, as long as (28) is fulfilled for identical Ri_{st}. Numerical examples with very different values of m and n confirmed indeed that the mixed layer depth depends only on Ri_{st}. This extends the findings of the authors mentioned above, who demonstrated that for all traditional models the mixed layer depth in the experiment of Kato and Phillips (1969) could almost perfectly be reproduced, provided the parameter $c_{\psi 3}$ was chosen to correspond to $Ri_{st} \approx 0.25$ (see Umlauf *et al.,* 2003). The proper choice of $c_{\psi 3}$ constitutes the fifth fundamental constraint; its definite value is

discussed in Section 4. Note, that in unstable situations, a different value of the parameter $c_{\psi 3}$ needs to be used. This does not cause a discontinuity in the model because the buoyancy term in (6) is zero at the transition between stable and unstable flows. An evaluation of the length-scale equations in convective flows, however, is intimately related to the third-order modelling of the triple correlation terms, a topic which is out of the scope of this paper.

So far, five of six possible constraints for the traditional models have been prescribed. We consider all of them to be fundamental for the class of models considered here. In the following section, we concentrate on steady-state, quasi shear-free, inhomogeneous turbulence, the only flow exhibiting a pure balance between turbulent transport and dissipation. This flow is of importance in oceanographic turbulence models, since it directly relates to some recently suggested models for turbulence generated by breaking gravity waves in lakes or in the ocean.

e. Shear-free turbulence

The first step in understanding the behaviour of two-equation models in the surface layer affected by breaking gravity waves is the investigation of a special case, in which turbulence decays spatially away from a source *without mean shear*. Turbulence generated by an oscillating grid in a water tank has been used in various laboratory settings to study the spatial decay of velocity fluctuations in this basic turbulent flow, where turbulent transport and dissipation balance exactly. Having the influence of grid generated turbulence on inter-facial mixing in stratified fluids in mind, pioneering works of this type were conducted by Thompson and Turner (1975) and Hopfinger and Toly (1976). Since their results were not entirely conclusive, a number of similar experiments followed until very recently (Hannoun *et al.,* 1988; Nokes, 1988; deSilva and Fernando, 1992; Cheng and Law, 2001).

A direct numerical simulation (DNS) of the transport-dissipation balance at low Reynolds numbers was performed by Briggs *et al.* (1996), who apparently were also the first to investigate the performance of some standard down-gradient models for the turbulent transport terms appearing in the balance equation of the Reynolds-stress tensor. These authors found that the models for the transport terms underpredict the measurements, but correctly reproduce the trends. Since the contraction of these (isotropic) transport models leads to an eddy-diffusivity model as in (11), we assume that the turbulent transport in shear-free turbulence is represented at least qualitatively correct in our model. For this reason, we confine ourself here to the transport model (11) and investigate the performance of the generic model (and other two-equation models) in this framework. The implications of model performance in shear-free turbulence will be compared to available data on breaking surface waves in Section 5.

All grid stirring experiments cited in Table 5 confirm a power law for the decay of k and a linear increase of the length scale l according to

$$k = K(z + z_0)^\alpha, \qquad l = L(z + z_0), \qquad (29)$$

Table 5. Decay exponent for the turbulent kinetic energy, α, and the constants of proportionality for the length-scale, L, in grid stirring experiments and DNS. The values in brackets have been calculated by assuming that the decay exponent for the horizontal velocity fluctuations is half of that for k.

Measured decay rates:	α	L
Thompson and Turner (1975)	$-(3.0)$	0.1
Hopfinger and Toly (1976)	-2.0	0.17–0.33
Nokes (1988)	$-(1.7–3.0)$	—
Hannoun *et al.* (1988)	$-(2.0)$	0.1
Briggs *et al.* (1996), DNS	-2.45	—
Cheng and Law (2001)	$-(2.0)$	0.06–0.2

where K, L, and z_0 are constants, and the source of turbulence has been assumed to be at $z = 0$. In these experiments, $z_0 = l/L$ at $z = 0$ is not related to any kind of surface roughness length. Rather, it is connected to the length scale of injected turbulence which is determined uniquely by the spectral properties of turbulence at the source. As already pointed out by Thompson and Turner (1975), the decay of k occurs with respect to the so-called *virtual origin* $z = -z_0$ which never coincides with the position of the source. In agreement with Hopfinger and Toly (1976), we define the virtual origin as the point, where the turbulent length-scale, l, becomes zero. It has been remarked by almost all authors that the decay coefficients are very sensitive with respect to small uncertainties in position of the virtual origin.

The values in Table 5 suggest that the decay rate for the turbulent kinetic energy is likely to be between $-3 < \alpha < -2$. The values of L, i.e. the slope of the turbulent length scale, l, indicate that in all cases $L < \kappa \approx 0.4$. Despite this fact, all previous authors adopted $L = \kappa$, which implies that length-scales in wall-bounded shear flows and in shear-free flows behave identically (Craig and Banner, 1994; Burchard, 2001b).

In stationary, shear-free, unstratified turbulence, the generic model simplifies to a balance between the turbulent transport terms and the dissipative terms in (1) and (6). Using the definition of ψ, (5), and the scaling for the rate of dissipation, (3), the transport and dissipation of k and ψ are balanced according to

$$
\frac{d}{dz}\left(\frac{c_\mu}{\sigma_k^\psi}k^{1/2}l\frac{dk}{dz}\right) = (c_\mu^0)^3\frac{k^{3/2}}{l},
$$

$$
\frac{d}{dz}\left(\frac{c_\mu}{\sigma_\psi}k^{1/2}l\frac{d}{dz}((c_\mu^0)^p k^m l^n)\right) = c_{\psi 2}(c_\mu^0)^{p+3}k^{m+(1/2)}l^{n-1}.
$$

(30)

Note, that in shear-free turbulence, the shear number is $S = 0$ by definition and stability functions always reduce to a constant which is, however, different from the constant c_μ^0 approached in the logarithmic boundary layer. It follows, e.g., from (26) that for the ASM of Canuto *et al.* (2001) this constant is $c_\mu = 0.107$.

Table 6. Constant of proportionality, L, for the turbulent length scale, l. Decay exponent, α, for the turbulent kinetic energy, β for the rate of dissipation, and γ for the turbulent diffusivity, as computed by different two-equations models. $\kappa = 0.4$ refers to the models calibrated with the help of (14) to compute this value of the von Kármán constant. $E_2 = 0$ refers to the model of MY82 without wall function.

Computed decay rates:	L	α	β	γ
W88	0.25	-2.53	-4.79	-0.26
W88, $\kappa = 0.4$	0.24	-2.68	-5.01	-0.34
MY82	0.16	-3.85	-6.78	-0.92
MY82, $E_2 = 0$	0.22	-2.87	-5.30	-0.43
R87, $\sigma_\epsilon = 1.3$	0.09	-4.97	-8.46	-1.49
R87, $\kappa = 0.4$	0.025	-17.78	-27.67	-7.89

For the solution of this nonlinear system, we inserted the expressions (29) in (30). From (3) and (10), power-laws follow then also for $\epsilon = E(z + z_0)^\beta$ and $\nu_t = N(z + z_0)^\gamma$. A similar method has already been used by Umlauf *et al.* (2003) to investigate the W88 model.

Inserting (29) into $(30)_1$ yields the equation

$$(\alpha L)^2 = \frac{2}{3}(c_\mu^0)^2 R \sigma_k^\psi, \tag{31}$$

where the constant ratio $R = c_\mu^0/c_\mu$ follows uniquely from the respective ASM. The power-law (29) can also be inserted in $(30)_2$ to yield

$$(\alpha m + n)\left(\left(\frac{1}{2} + m\right)\alpha + n\right)L^2 = (c_\mu^0)^2 R \sigma_\psi c_{\psi 2}. \tag{32}$$

The physical meaningful roots of (31) and (32) are

$$\alpha = -\frac{4n(\sigma_k^\psi)^{1/2}}{(1 + 4m)(\sigma_k^\psi)^{1/2} - (\sigma_k^\psi + 24\sigma_\psi c_{\psi 2})^{1/2}},$$

$$L = c_\mu^0 R^{1/2}\left(\frac{(1 + 4m + 8m^2)\sigma_k^\psi + 12\sigma_\psi c_{\psi 2} - (1 + 4m)(\sigma_k^\psi(\sigma_k^\psi + 24\sigma_\psi c_{\psi 2}))^{1/2}}{12n^2}\right)^{1/2}. \tag{33}$$

For the standard models (without ASM), $R = 1$ may be assumed. Then, with the values of m and n from Table 1 and the model parameters from Table 2, solutions for the k-ϵ model of R87, and the k-ω model of W88 can be directly recovered as special cases of this equation. The solution for the MY82 (not shown) is slightly more complicated because of the presence of the wall-function. Predicted decay rates for the turbulent quantities are listed in Table 6. Comparison with the measured values in Table 5 reveals that of the classical models only the model of W88 reproduces correct decay rates. The decay predicted by the R87 is much too strong and, as illustrated in Figure 1, extremely sensitive
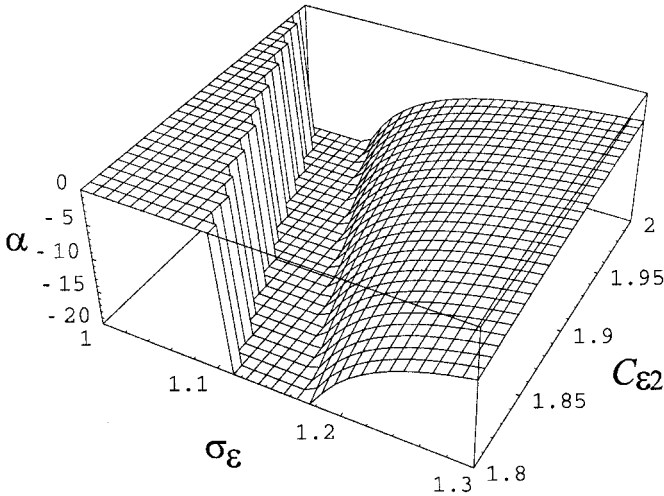
Figure 1. Decay exponent, α, of the R87 model in shear-free turbulence as a function of the model parameter σ_ϵ and $c_{\epsilon 2}$ according to (33)$_1$. For clarity, the exponents are cut off for $\alpha < -20$ and $\alpha > 0$. The singularity of α is indicated by the vertical surface in the plot. The standard values are $\sigma_\epsilon = 1.3$ and $c_{\epsilon 2} = 1.92$. The value $\sigma_\epsilon = 1.11$ corresponds to $\kappa = 0.4$ according to Table 3.

with respect to small changes in the parameters. In addition, the denominator in the expression for α in (33) may become zero for certain parameters inside the range of those most commonly used. Then, the decay rate becomes infinite (see Fig. 1). For the standard parameters of the R87 model, this 'singularity' occurs at $\sigma_\epsilon = \sigma_\epsilon^{\text{crit}} \approx 1.042$. For smaller values of this parameter, model results become unphysical (see Section 5). The model of MY82 predicts different decay rates depending on the influence of its wall-function. This implies, quite unphysically, that the predicted decay for the same physical process depends on the vertical position of its occurrence in the water column.

A more detailed discussion can be found in Umlauf *et al.* (2003). Some numerical results are presented in Section 5.

4. Model calibration and polymorphism

Recall from the discussion in Section 3 that five of the six model parameters have already been chosen to satisfy some fundamental constraints. Only one parameter is left: The Schmidt number for the turbulent kinetic energy, σ_k^ψ. Since σ_k^ψ appears in both equations of (33), either α or L can be adjusted to the measured values by varying this parameter, but not both. After assigning a definite value to σ_k^ψ, the calibration possibilities of the traditional models are exhausted and the value of the second quantity follows automatically, and, regrettably, not in conformance with the measurements in most cases. Any attempt of calibrating both, α and L, will inevitably violate one of the fundamental constraints mentioned above.

Table 7. Some parameter sets for the generic model with $\kappa = 0.4$, $d = -1.2$, $(c_\mu^0)^2 = 0.3$, $c_{\psi_1} = m$ and the log-layer compatibility relation, (27).

α	L	m	n	c_{ψ_2}	σ_k^ψ	σ_ψ
-2.0	0.20	1.00	-0.67	1.22	0.80	1.07
-2.0	0.20	2.00	-1.09	2.36	0.80	1.75
-2.5	0.20	1.00	-1.05	1.35	1.25	1.68
-2.5	0.20	2.00	-1.74	2.58	1.25	2.78

To overcome this problem, we propose to make use of the polymorphic nature of the generic model and consider the *structure* of the two-equation model itself for calibration. Accepting this point of view, two new 'model parameters', the exponents m and n defined in (5), become available.

a. Model groups with common properties

The new approach is best demonstrated with an example. Supposed, we decide to prescribe (inspired from Table 5) the values $\alpha = -2.0$ and $L = 0.2$ in shear-free turbulence, without touching any of the constraints mentioned earlier. Then, from (31) it follows immediately that $\sigma_k^\psi = 0.8$ ($R = 1$ is assumed here for simplicity). Recall, that $(c_\mu^0)^2 \approx 0.3$, also appearing in (31), is dictated from the fundamental constraint (13) and should not be changed significantly.

Inserting the constraints (16) and (27) in (32), an equation expressing the exponent m in terms of n (or vice-versa) can be obtained. The result for n can be written as

$$n = -\frac{1}{4(2 + d)(\kappa^2 R - L^2)} (4d\kappa^2 Rm - (1 + 4m)(2 + d)\alpha L^2$$
$$+ \sqrt{8m(1 + 2m)(2 + d)^2(\kappa^2 R - L^2)\alpha^2 L^2 + (-4d\kappa^2 Rm + (2 + d)(1 + 4m)\alpha L^2)^2}).$$
(34)

After assigning appropriate values for the von Kármán constant, κ, the decay coefficient of homogeneous turbulence, d, the spatial decay rate, α, and the slope, L, an infinite number of pairs of m and n satisfying (34) can be derived. Each corresponds to a different two-equation model. Some example are given in Table 7.

Even though each line in this table represents a different two-equation model with completely different model constants, each of the two groups of models (with $\alpha = -2.0$ and $\alpha = -2.5$, respectively) *performs completely identical in all situations discussed until here.* Thus, the generic model allows for the formulation of groups of two-equation models with fully controlled properties from the outset. Figure 2 illustrates this fact graphically. Each curve in this figure represents a solution of (34) for a given set of constraints as indicated in the caption. Models corresponding to these curves perform *identically* in all standard situations with α and L as indicated. However, the models may exhibit a different
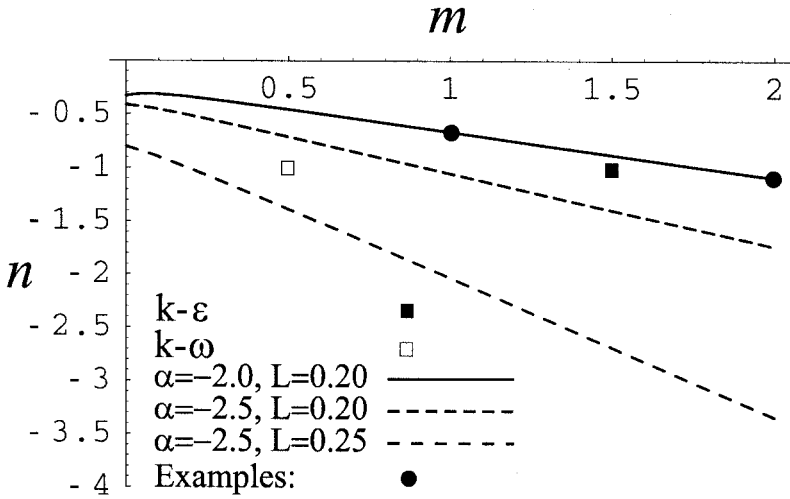
$$m$$

Figure 2. Graphical presentation of model groups that behave identically in the standard situations with $\kappa = 0.4$, $d = -1.2$, $(c_\mu^0)^2 = 0.3$, $c_{\psi_1} = m$ and the log-layer compatibility relation, (27). Also displayed are the positions of the k-ϵ model and the k-ω model. The dots mark two models that were integrated numerically (see Section 5).

behaviour in other situations not discussed yet. Applying the model to one more *independent* constraint amounts to the selection of one point on each of the curves. In this sense, the generic model can be regarded as a tool to objectively determine an optimal two-equation model for a certain set of constraints.

Finally, it should be remarked that, from Section 3d, the steady-state Richardson number Ri_{st} has to re-computed for each new combination of a two-equation model and an ASM. Evidently, we cannot present all possible combinations here. However, Table 8 gives some examples for the ASM of Canuto *et al.* (2001), combined with a number of well-known models (including the generic model with $m = 1$ corresponding to the first line of Table 7, which will be our final recommendation). Numerical tests with these models demonstrated that the mixed layer depth predicted for the experiment of Kato and Phillips (1969) were almost identical to the experimental results, if the value $Ri_{st} = 0.25$ was adopted (also see Umlauf *et al.*, 2003).

Table 8. Value of the model constant $c_{\psi 3}$ corresponding to $Ri_{st} = 0.25$ computed from (28) for different models and the ASM of Canuto *et al.* (2001). 'Generic' corresponds to the first line of Table 7.

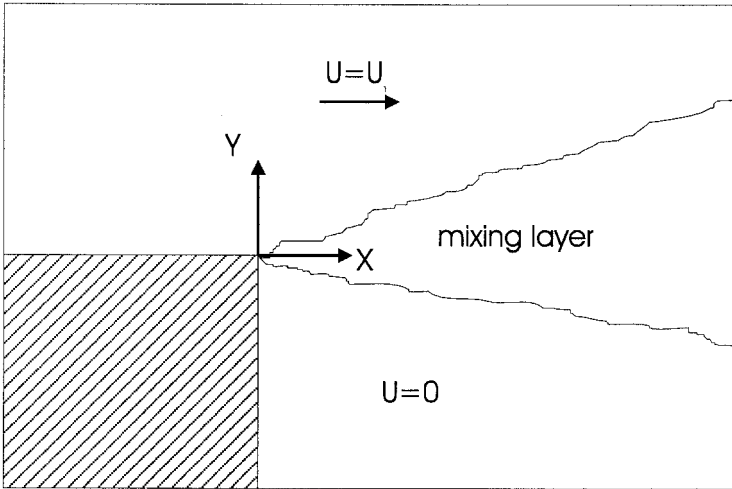| MY82	R87	W88	Generic ($m = 1$)
2.62	-0.629	-0.642	0.05

Figure 3. Geometry of the turbulent mixing layer for a flow with $u = U_1$ in the upper layer and $u = 0$ in the lower layer.

b. Plane mixing-layer

To find a final constraint with a certain generality, we considered a turbulent plane mixing layer without stratification. Among other classical flows like the turbulent wake and jet, we felt that the plane mixing layer is of greatest relevance in oceanic situations. The geometry of this flow is sketched in Figure 3. Numerous experimental investigations confirmed the self-similarity of this flow, in which statistical quantities depend only on the similarity variable η defined as

$$\eta = \frac{y}{\delta(x)}, \tag{35}$$

where, according to all measurements, the function $\delta(x)$ is linear in x.

Interestingly, the group of models considered here also exhibits a self-similar solution for this flow, and thus can directly be compared to the measurements. The transformation of the governing equations into self-similar form is, however, somewhat tedious and cannot be demonstrated here in full detail. An exhaustive discussion of the general procedure can be found in some textbooks on turbulence (see Wilcox, 1998).

The first step is to re-write the statistical quantities in the plane mixing-layer in self-similar form. The velocity for example is expressed as

$$u = U_1 \mathcal{U}(\eta), \tag{36}$$

where U_1 is the velocity in the upper part of mixing layer for $y \to \infty$ (see Fig. 3). The turbulent kinetic energy, k, and the length scale, l, are expressed in self-similar form as

$$k = \mathcal{K}(\eta) U_1^2, \qquad l = \mathcal{L}(\eta)\delta. \tag{37}$$

With the help of (3), (5), and (10), expressions for ψ, ϵ, and ν_t, can be written as

$$\psi = \mathcal{P}(\eta) U_1^{2m}\delta^n, \qquad \epsilon = \mathcal{E}(\eta) U_1^3 \delta^{-1}, \qquad \nu_t = \mathcal{N}(\eta) U_1 \delta, \tag{38}$$

respectively.

Using the above expressions, the governing equations for the mean and turbulent quantities can be transformed into self-similar form, provided $\delta = x$ is identified in accordance with the experiments. The balance of momentum can then be reformulated as

$$\mathcal{Q}\mathcal{U}' = (\mathcal{N}\mathcal{U}')', \tag{39}$$

where the primes denote derivatives with respect to η, and

$$\mathcal{Q} = -\int_0^\eta \mathcal{U}d\eta \tag{40}$$

has been introduced for convenience.

Similarly, equations for the turbulent kinetic energy,

$$\mathcal{Q}\mathcal{K}' = \mathcal{N}\mathcal{U}'^2 + \left(\frac{\mathcal{N}}{\sigma_k^\psi}\mathcal{K}'\right)' - \mathcal{E}, \tag{41}$$

and the generic length scale,

$$n\mathcal{P}\mathcal{U} + \mathcal{Q}\mathcal{P}' = \frac{\mathcal{P}}{\mathcal{K}}(c_{\psi 1}\mathcal{N}\mathcal{U}'^2 - c_{\psi 2}\mathcal{E}) + \left(\frac{\mathcal{N}}{\sigma_\psi}\mathcal{P}'\right)', \tag{42}$$

can be obtained from (1) and (6).

We iteratively solved the nonlinear set of equations (39)–(42) with a finite-volume method on a staggered grid. The results for the model of MY82 (without wall-function), the model of R87, and the model of W88 are presented in the left panel of Figure 4. All models have been used in their 'standard' versions with constant c_μ. It can be seen that the models roughly follow the classical data-set of Liepmann and Laufer (1947). Evidently, however each model fails at either the upper or the lower end of the mixing layer. In particular, these models predict a sharp interface between the turbulent and non-turbulent regions at the ends of the mixing layer. Even though it is true that the *instantaneous* interface is sharp, the same is not true for its average position as clearly indicated by the data of Liepmann and Laufer (1947). Above this, a sharp interface may lead to serious numerical inaccuracies (see Wilcox (1998)).

Results for the generic model with $m = 1$ and $m = 2$, corresponding to the first and second line in Table 7, are displayed in the right panel of Figure 4. The spreading rate of the plane mixing layer is clearly underpredicted by the model with $m = 2$. However, with $m =$
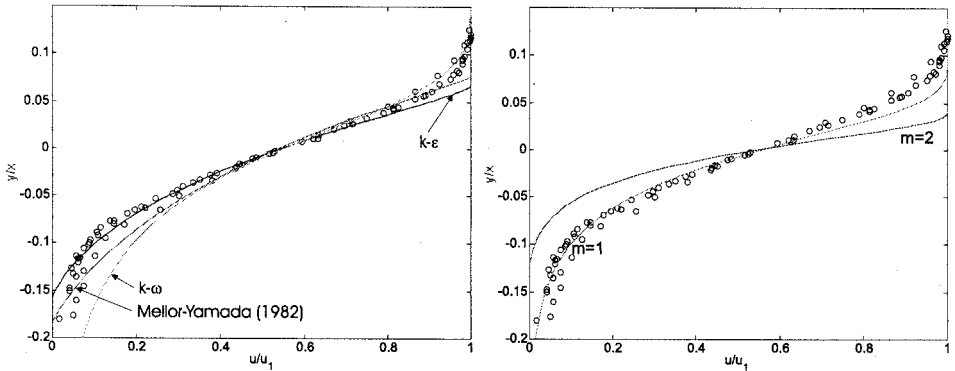
Figure 4. Numerical solutions of (39)–(42) compared to the data of Liepmann and Laufer (1947). Left panel: The traditional models of MY82, R87, and W88. Right panel: The generic model with $m = 1$ and $m = 2$ according to the first two lines in Table 7.

1 the fit to the data is satisfying and at least as good as any of the traditional models, and also the problem with the sharp mixing layer interface is avoided.

We therefore recommend this parameter set (including the parameter $c_{\psi 3}$ discussed in the previous section), which yields a two-equation model with almost fully controlled properties for a great range of typical oceanic flows.

5. Discussion

Since the correct behavior of the generic model in standard situations (logarithmic boundary layer, decay of homogeneous turbulence, etc.) is asserted by the calibration procedure in Section 3, we discuss here the more specific case of a free surface flow with strong wind forcing and breaking waves.

It has been shown in numerous studies (Kitaigorodskii *et al.,* 1983; Thorpe, 1984; Osborn *et al.,* 1992) that the simple assumption of a logarithmic law-of-the-wall flow very close to the surface does not hold under breaking waves. Using state-of-the-art measuring techniques, recent publications (Anis and Moum, 1995; Terray *et al.,* 1996; Gemmrich and Farmer, 1999; Terray *et al.,* 1999) suggested more refined models for the effects of wave breaking and, in addition, proposals for the vertical distribution of the dissipation rate, $\epsilon(z)$, in the upper few meters in the ocean and in lakes. The results obtained by these authors, however, exhibit a large scatter, and at present one has to conclude that the mechanics of the wave breaking problem are not fully understood.

Nevertheless, there appears to be an agreement upon the following points:

(1) Turbulence is produced in a thin 'breaking layer.' Its thickness may be comparable to the significant wave height, H_s, if waves break (Terray *et al.,* 1996). Some authors, however, find much smaller values (Gemmrich and Farmer, 1999). (2) Below this layer, turbulence is dominated by the balance between dissipation and turbulent transport of

turbulent kinetic energy introduced in the 'breaking layer.' In this 'transport layer,' the rate of dissipation probably decays according to a power law. (3) Below the wave affected layer, where shear production becomes increasingly important, a flow region with a logarithmic velocity distribution exists.

Since little is known about the production mechanisms in the uppermost 'breaking layer', we model the turbulent energy source simply by a flux boundary condition of the form

$$\frac{\nu_t}{\sigma_k}\frac{\partial k}{\partial z} = -\eta u_*^3, \tag{43}$$

where u_* is the surface friction velocity and $\eta \approx 100$ an empirical model constant. The minus sign accounts for the fact that k decreases away from the surface. This model was suggested by Craig and Banner (1994). Its basic assumptions were later confirmed by Terray *et al.* (1996), at least for a fully developed wave field. Since we assume that the thickness of the 'breaking layer' is of the order of H_s (see Terray *et al.,* 1996), there is some ambiguity about the precise position where (43) should be applied. In our case, $z = 0$ refers to the bottom of the unresolved 'breaking layer' and *not* to the water surface as e.g. in Terray *et al.* (1996, 1999).

In the transport layer, the class of turbulence models presented here should predict power-laws according to the shear-free solutions (see Section 3e), provided the local shear-production is in fact negligible. However, due to the wind stress, velocity shear in the upper part of the water column will always be present under breaking surface waves, and it has to be examined to what extent the shear-free solutions presented above retain their applicability.

In the models, the influence of the mean shear manifests itself in two ways: via the shear production, P, and via the shear-number S appearing in (26). In that sense, the shear-number is a structure parameter describing the relative influence of the mean shear on the transport of turbulence away from the 'breaking layer.'

To derive an expression for the shear-number in the 'transport layer,' we postulate that the power laws (29) remain approximately valid even when shear caused by the wind-stress is present. We will have to justify this assumption *a-posteriori*. To compute an expression for the velocity gradient, recall first that the balance of momentum in a stationary horizontal boundary layer without pressure-gradient simplifies to

$$\nu_t \frac{\partial u}{\partial z} = -u_*^2, \tag{44}$$

where the unusual minus sign is due to the fact that the velocity actually decreases away from the free surface (positive z). This equation is valid even with injection of k according to (43). Substituting the power-laws (29) in (10), (44) can be solved for the velocity gradient needed to compute S. We want to remark that by integrating the expression for the

velocity gradient, it can be shown that the velocity decays according to a power law with slope $-\alpha/2$.

With the help of (29), (3), and the parameterisation (43), a short calculation yields then

$$S = \left(\frac{2}{3}\right)^{1/3} ((c_\mu^0)^3 c_\mu \eta (\sigma_k^\psi)^{1/2})^{-2/3} \left(\frac{z + z_0}{z_0}\right)^{-\alpha} < 0.25 \left(\frac{z + z_0}{z_0}\right)^{-\alpha}, \tag{45}$$

where the last inequality holds for all models considered here. Remarkably, the shear number S does not depend on the normalized surface shear, u_*^2, which is a direct consequence of the cubic dependence of the flux of k on u_* in (43). S increases slowly away from the surface but remains small compared to $S \approx 3.5$ in the log layer or $S \approx 5$ in homogeneous shear-flows provided z does not exceed a few times H_s, since z_0 is of the order of H_s (see Terray *et al.,* 1996; 1999). From (26) it follows then that c_μ is very close to the shear-free value $c_\mu = 0.107$, and the shear-free solutions (33) remain a good approximation also in the case with $u_* \neq 0$, i.e. in the wave-breaking case.

This interesting result states that a typical Reynolds-stress model predicts the mean shear to affect the structure of turbulence in the 'transport layer' only marginally. However, if z exceeds a few times H_s, the shear-number may be large. But then also the shear-production becomes significant and the shear-free solutions loose their validity always.

Clearly, this scenario relies on the concept of some 'small-scale' turbulence injected by breaking waves in the presence of some 'large-scale' turbulence caused by local shear production. Effects of large coherent structures ('Langmuir-circulation') may also be of importance, but their effects on turbulent transport in the mixing layer are just beginning to be understood, and currently no useful models exist for their inclusion into a Reynolds-stress model of the type described here (see Thorpe *et al.,* 2003).

a. Idealized test cases

The generic model was implemented and solved numerically with a finite-volume technique on a staggered grid. The resolution was in all cases fine enough to exclude any dependence of the results on grid spacing. We considered the problem of spatially decaying turbulence along the coordinate direction z from a planar source at $z = 0$ with and without a constant shear stress applied at $z = 0$. The flux of k was computed according to (43). All results refer to the stationary case. The model runs were conducted for two different parameter sets corresponding to the first and second parameter set given in Table 7 (with $m = 1$ and $m = 2$). For comparison, also the results of the k-ϵ model are discussed.

The left panel of Figure 5 illustrates the increase of the integral scale, l, with increasing distance from the source in non-dimensional form. It is evident that in the shear-free cases this scale increases linearly with a slope $L = 0.2$, just as predicted by the theory (see Table 7). A remarkable feature of these profiles is the virtual collapse of profiles computed with two different models corresponding to $m = 1$ and $m = 2$ in Table 7. This was to be expected from the theory.

Wave breaking corresponds to the more realistic case with a surface shear stress added at
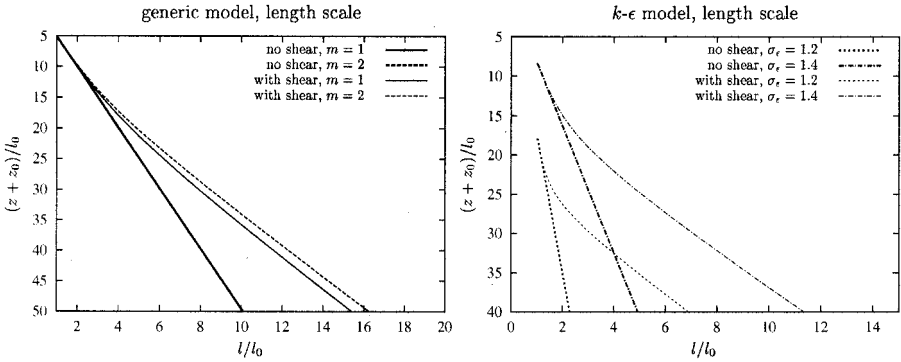
Figure 5. Left panel: Dimensionless representation of the turbulent length scale, l, with distance z from the source for the first two models from Table 7 with and without a constant shear at $z = 0$. Right panel: Same as left panel, but now for the standard k-ϵ model with different values of σ_ϵ.

$z = 0$. Then, the model still predicts a boundary layer for $(z + z_0)/l_0 < 10$ (the 'transport layer'), in which shear production is small compared to dissipation, and l behaves according to the shear-free case. Below this layer (and a small transition region), the slopes of the length-scales in both cases rapidly approach $\kappa = 0.4$, an indication for the existence of a logarithmic layer (see below). The k-ϵ model, displayed in the right panel of Figure 5 for two values of the model constant σ_ϵ in the neighborhood of the standard value $\sigma_\epsilon = 1.3$ exhibits a similar behaviour. In accordance with the values of L in Table 7, the length scale increases much slower than that of the generic model and, in fact, too slowly compared to the measured values from Table 5.

Profiles of the turbulent kinetic energy, k, for the same situation are displayed in Figure 6. The left panel of this figures reveals that in the shear-free case the generic model almost perfectly predicts a slope of $\alpha = -2$ and coinciding profiles for $m = 1$ and $m = 2$ (as required for the first two models in Table 7). For the cases with shear, again a boundary layer for $(z + z_0)/l_0 < 10$ develops, in which the profiles coincide with those of the
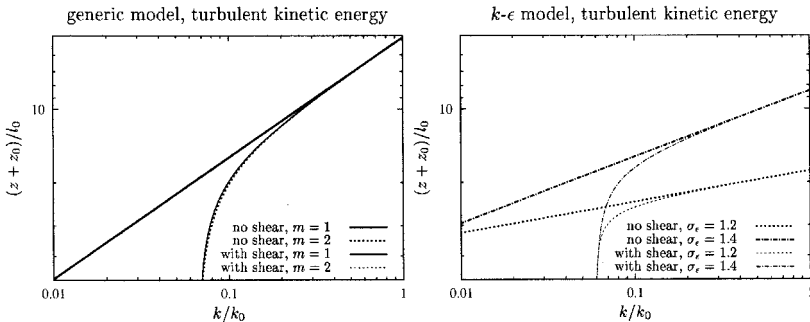

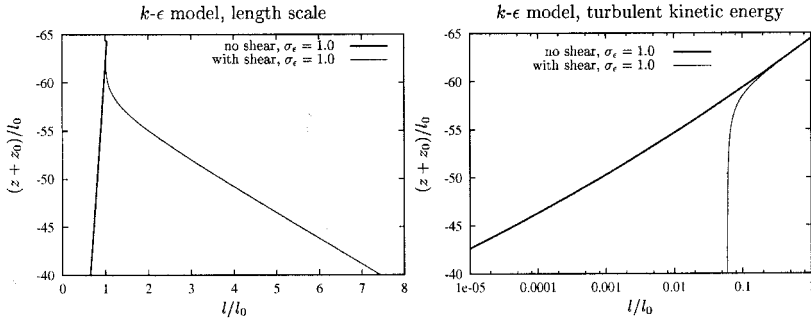Figure 6. Same as in Figure 5, but now for the turbulent kinetic energy, k.

Figure 7. Same as the right panels in Figure 5 and Figure 6, but now for the case with $\sigma_\epsilon = 1.0$. The negative values of the ordinate result from the fact that the virtual origin $z = -z_0$ is reversed due to the negative slope of the length scale, L.

shear-free cases. Below this layer, k tends to become constant, another indication for the existence of a logarithmic region. The k-ϵ model, displayed on the right panel of this figure, exhibits in principle a similar behaviour, even though for this model the decay is too rapid compared to the measured values and is, as evident from the figure, also very sensitive with respects to small changes in the model parameter σ_ϵ (see Table 6).

The left panel of Figure 7 illustrates the numerical consequence of the singular behavior of the k-ϵ model: In the shear-free case, for $\sigma_\epsilon < \sigma_\epsilon^{crit} = 1.042$ the length-scale tends to *decrease* with increasing distance from the source, in contrast to all measurements. For $\sigma_\epsilon = 1.0$, the decay of k, displayed in the right panel of Figure 7, does not conform to a power-law. Due to the decreasing length-scale and the rapid decay of k, mixing is strongly suppressed, even for small values of z. The cases with a constant shear stress at $z = 0$ are analogous to the previous results and the undesired behaviour of the k-ϵ model beyond the singularity is confined to the wave-affected boundary layer.

The structure of the velocity profile resulting from a constant shear and injection of k at $z = 0$ is investigated in Figure 8 for the generic model with $m = 1$ and $m = 2$. The left panel of this figure focuses on the upper layer with an approximate transport-dissipation balance. Recall that it was remarked above that from the analytical solutions it can be shown that the velocity decays according to a power law with slope $-\alpha/2$. Since in this example we use $\alpha = -2$ (see Table 7), the velocity must decrease linearly in the 'transport layer', and this is in fact observed in the left panel of Figure 8 for values smaller than $(z + z_0)/z_0 \approx 4$.

A slope of $\kappa = 0.4$ for the integral scale, l, and the constancy of k are strong indicators for the existence of a logarithmic velocity profile below the transport-dominated boundary layer. Then, the velocity should decay logarithmically according to

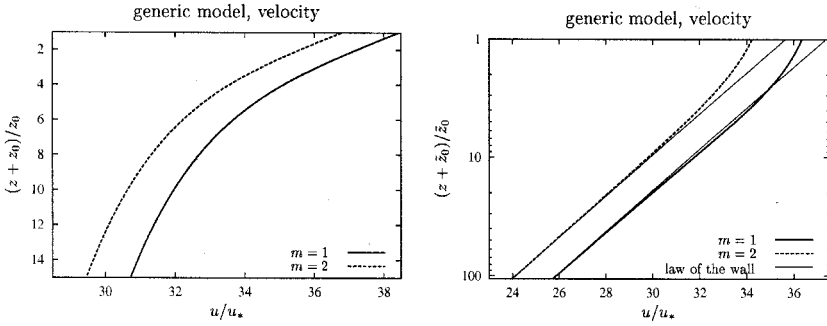$$u = -\frac{u_*}{\kappa} \log \frac{z + \bar{z}_0}{\bar{z}_0} + c, \tag{46}$$

Figure 8. Dimensionless plot of the mean velocity, v, with distance, z, from the source. A constant shear is applied at $z = 0$. Left panel: Linear scaling with z_0. Right panel: Logarithmic scaling with $\bar{z}_0$.

where c denotes an unknown constant determined by the outer region of the flow. The quantity $\bar{z}_0$ is usually referred to as the roughness length in this context. However, since here the properties of the turbulence at the surface are set exclusively by its source, $\bar{z}_0$ cannot be related to any kind of 'roughness' in the classical sense. The value of $\bar{z}_0$ was found by extrapolating the part of the profile with slope equal to κ in the left panel of Figure 5 to the point, where it intersects the (nondimensional) z-axis[11]. The right panel of Figure 8 illustrates that the velocity profile indeed closely follows the predicted form of (46), provided u is made dimensionless with quantities relevant to the logarithmic layer. This panel also suggests that enhanced turbulence due to breaking waves leads to a reduction of the surface speed with respect to the logarithmic velocity profile. This corresponds to measurements in the upper layer discussed in Terray *et al.* (1999) and Umlauf *et al.* (2003).

b. Surface wave breaking

In this final section, profiles of the dissipation rate ϵ as computed by the generic two-equation model are compared to observations of micro-structure under wind-driven, breaking surface waves in oceans and lakes. As already discussed before, this flow is a generalization of pure shear-free turbulence.

Detailed measurements in the 'transport layer' demonstrated that the turbulent dissipation rate decays approximately according to a power law with slopes between $\beta = -2.7$ and $\beta = -1.9$, in contrast to a slope of -1 for the logarithmic law (see e.g. Terray *et al.*, 1996; Drennan *et al.*, 1996; Anis and Moum, 1995). This is not necessarily in contradiction with the laboratory observations compiled in Table 5, suggesting $-5.55 < \beta < -3.55$ from (3), since in both cases a different origin has been used. It has been by pointed out by Terray *et al.* (1996) that even though their data suggest a decay rate of $\beta \approx -2$ (with

---

11. An analytical expression for the position of $\bar{z}_0$ can only be found by solving the full set of model equations in steady-state, and such a solution is not available yet.
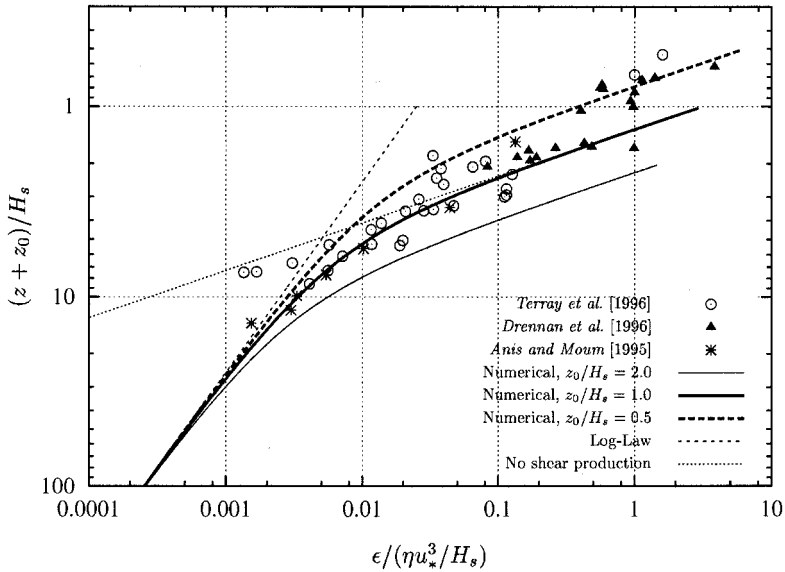
Figure 9. Observations and simulations of turbulent dissipation rate in the wave-enhanced layer. The observations of Terray *et al.* (1996), Drennan *et al.* (1996) and Anis and Moum (1995) are normalized by surface TKE flux and significant wave height, see Terray *et al.* (1999). The simulations have been carried out with the generic model surface length scale $z_0 = l_0/L$ to wave height H_s ratios of 2.0, 1.0 and 0.5. For comparison, the logarithmic law and the shear-free case have been included. The empirical constant $\eta = 100$ is the coefficient of proportionality for relating the surface flux of turbulent kinetic energy to the cubed friction velocity, u_*.

respect to the surface), they compare well to the model of Craig and Banner (1994) with $\beta = -3.4$ (with respect to the virtual origin, where $l = 0$), if they are plotted with respect to *the same* origin. To achieve agreement of the two origins, we compare models and data by referring to the origin $z = 0$ located at the bottom of the 'breaking layer' (see above).

Terray *et al.* (1999) displayed various oceanic measurements in one graph, non-dimensionalised by the observed significant wave height, H_s, and the surface friction velocity, u_*, and found that the data reasonably collapsed into one curve. To reproduce the trends in these data, Burchard (2001b) investigated a k-ϵ model with modified turbulent Schmidt number, σ_ϵ, yielding a decay rate of $\beta = -2.68$ for the dissipation rate. Using the same origin suggested also here, he was able to reproduce the data of Terray *et al.* (1999) well for $z_0/H_s = 0.5$. However, this modified k-ϵ model was based on the assumption $L = \kappa = 0.4$ always, which is evidently not supported by laboratory experiments compiled in Table 5.

We used the generic model with $\beta = -4$, $L = 0.2$, and $\kappa = 0.4$ to reproduce the data compiled by Terray *et al.* (1999). The results are illustrated in Figure 9, which demonstrates that most of the data are fitted well for $z_0 = H_s$, even somewhat different choices for z_0/H_s are conceivable. Only near the surface for $z + z_0 \lesssim H_s$ the observations are not

met very well for $z_0 = H_s$. However, this region belongs to the 'breaking layer,' which is not resolved in our model by definition, and hence agreement cannot be expected.

Given all the uncertainties, we claim that the generic two-equation model yields reasonable estimates of enhanced turbulence under breaking surface waves. However, as already pointed out by Craig (1996), the major remaining problem is to estimate the length-scale, z_0, or the relevant scale of turbulence under breaking waves.

6. Conclusions

We discussed the properties of a family of differential length-scale equations typically used in marine Reynolds-stress models of turbulent flows. A general framework for these equations was suggested, from which the most well-known ocean turbulence models can be directly recovered as special cases: The k-kl model of MY82, the k-ϵ model of R87, and the extended k-ω model of Umlauf *et al.* (2003).

This general framework for the length-scale equation can be regarded as both, a useful tool to analyse existing models and a generalized model equation on its own, with free parameters to be determined. We investigated both aspects.

The analysis of traditional models illustrated that they perform comparably in the classical standard flows, where production equals dissipation. However, in accordance with earlier findings of Umlauf et al. (2003), it was demonstrated that in shear-free situations, where the rate of dissipation is balanced by turbulent transport from an infinite planar source (e.g. a field of breaking surface waves), all models except the model of W88 fail. Even though this model appears to be the most generally applicable from a theoretical point of view, it is known to exhibit an extreme sensitivity with respect to the prescribed freestream value of turbulent quantities in free shear-flows (mixing layer, free jet, wake). This problem, which has not been discussed here, has been extensively investigated by Menter (1992) and Wilcox (1998). In addition, even though all of the traditional models predicted roughly the correct spreading rates for the unstratified plane mixing layer, they had difficulties in reproducing the correct profiles close to the edges.

In contrast, the generic length-scale equation, with parameters chosen in the way suggested here, is free of these problems. We showed how the framework of this equation can be used to derive a turbulence model with maximum control of its properties: After choosing reasonable values for *physically* significant key parameters, i.e. the von Kármán constant, κ, the homogeneous decay rate, d, the spatial decay rates, α and L, and the steady-state Richardson number, Ri_{st}, all model parameters are fixed. In addition, the set of analytical solutions of the generic model presented here offers useful insight into the fragile inter-dependence of the model parameters. With these parameters, the model will also perform satisfactorily in homogeneous stratified shear-flows, predict the correct mixed layer depth in stratified flows, and yield the correct spreading rate in unstratified plane mixing layers. These properties, which are of crucial importance in many oceanic situations, cannot all be shared by any of the traditional models. We want to remark that this fact, evidently, does not imply that the generic model will never fail. We think,

however, that, given the level of complexity of the models we discussed, the generic model is optimal in many marine situations.

Finally, it should be pointed out that, once the generic model is implemented in a numerical code, each of the traditional models can be recovered by simply changing a few parameters. There are virtually no computational extra costs compared to the traditional models.

REFERENCES

Anis, A. and J. N. Moum. 1995. Surface wave-turbulence interactions: Scaling $\epsilon(z)$ near the sea surface. J. Phys. Meteor., *25,* 2025–2045.

Baumert, H. and H. Peters. 2000. Second-moment closures and length scales for weakly stratified turbulent shear flows. J. Geophys. Res., *105,* 6453–6468.

Bradshaw, P. 1975. An Introduction to Turbulence and its Measurement, Pergamon, 218 pp.

Briggs, D. A., J. H. Ferziger, J. R. Koseff and S. G. Monismith. 1996. Entrainment in a shear-free turbulent mixing layer. J. Fluid Mech., *310,* 215–241.

Burchard, H. 2001a. Note on the $q^2 l$ equation by Mellor and Yamada [1982]. J. Phys. Oceanogr., *31,* 1377–1387.

—— 2001b. Simulating the wave-enhanced layer under breaking surface waves with two-equation turbulence models. J. Phys. Oceanogr., *31,* 3133–3145.

Burchard, H. and K. Bolding. 2001. Comparative analysis of four second-moment turbulence closure models for the oceanic mixed layer. J. Phys. Oceanogr., *31,* 1943–1968.

Burchard, H. and O. Petersen. 1999. Models of turbulence in the marine environment—a comparative study of two-equation turbulence models. J. Mar. Syst., *21,* 29–53.

Burchard, H., O. Petersen and T. P. Rippeth. 1998. Comparing the performance of the Mellor-Yamada and the $k - \epsilon$ two-equation turbulence models. J. Geophys. Res., *103,* (C5), 10,543–10,554.

Canuto, V. M., A. Howard, Y. Cheng and M. S. Dubovikov. 2001. Ocean turbulence. Part I: One-point closure model—momentum and heat vertical diffusivities. J. Phys. Oceanogr., *31,* 1413–1426.

Cheng, N.-S. and A. W.-K. Law. 2001. Measurements of turbulence generated by oscillating grid. J. Hydr. Eng., *127,* 201–208.

Craig, P. D. 1996. Velocity profiles and surface roughness under breaking waves. J. Geophys. Res., *101,* 1265–1277.

Craig, P. D. and M. L. Banner. 1994. Modeling wave-enhanced turbulence in the ocean surface layer. J. Phys. Oceanogr., *24,* 2546–2559.

deSilva, I. P. D. and H. J. S. Fernando. 1992. Some aspects of mixing in a stratified turbulent patch. J. Fluid Mech., *240,* 601–625.

Domaradzki, J. A. and G. L. Mellor. 1984. A simple turbulence closure hypothesis for the triple velocity correlation functions in homogeneous isotropic turbulence. J. Fluid Mech., *140,* 45–61.

Drennan, W. M., A. A. Donelan, E. A. Terray and K. B. Katsaros. 1996. Oceanic turbulence dissipation rate measurements in SWADE. J. Phys. Oceanogr., *26,* 808–815.

Galperin, B., L. H. Kantha, S. Hassid and A. Rosati. 1988. A quasi-equilibrium turbulent energy model for geophysical flows. J. Atmos. Sci., *45,* 55–62.

Gemmrich, J. R. and D. M. Farmer. 1999. Near-surface turbulence and thermal structure in a wind-driven sea. J. Phys. Oceanogr., *29,* 480–499.

Gerz, T., U. Schumann and S. E. Elghobashi. 1989. Direct numerical simulation of stratified homogeneous turbulent shear flows. J. Fluid Mech., *200,* 563–594.

Hannoun, I. A., H. J. S. Fernando and E. J. List. 1988. Turbulence structure near a sharp density interface. J. Fluid Mech., *189,* 189–209.

Holt, S. E., J. R. Koseff and J. H. Ferziger. 1991. A numerical study of the evolution and structure of homogeneous stably stratified sheared turbulence. J. Fluid Mech., *237,* 499–539.

Hopfinger, E. J. and J. A. Toly. 1976. Spatially decaying turbulence and its relation to mixing across density interfaces. J. Fluid Mech., *78,* 155–175.

Jacobitz, F. C., S. Sarkar and C. W. van Atta. 1997. Direct numerical simulations of the turbulence evolution in a uniformly sheared and stably stratified flow. J. Fluid Mech., *342,* 231–261.

Kaltenbach, H.-J., T. Gerz and U. Schumann. 1994. Large-Eddy simulation of homogeneous turbulence and diffusion in stably stratified shear flow. J. Fluid Mech., *280,* 1–40.

Kato, H. and O. M. Phillips. 1969. On the penetration of a turbulent layer into stratified fluid. J. Fluid Mech., *37,* 643–655.

Kitaigorodskii, S. A., M. A. Donelan, J. L. Lumley and E. A. Terray. 1983. Wave turbulence interactions in the upper ocean. Part II: Statistical characteristics of wave and turbulent components of the random velocity field in the marine surface layer. J. Phys. Oceanogr., *13,* 1988–1999.

Liepmann, H. W. and J. Laufer. Investigations of free turbulent mixing. Technical Report 1257, N.A.C.A., 1947.

Mellor, G. L. and T. Yamada. 1974. A hierarchy of turbulence closure models for planetary boundary layers. J. Atmos. Sci., *31,* 1791–1806.

—— 1982. Development of a turbulence closure model for geophysical fluid problems. Reviews of Geophysics and Space Physics, *20,* 851–875.

Menter, F. R. 1992. Influence of freestream values on k-ω turbulence model predictions. AIAA J., *30,* 1657–1659.

Mohamed, M. S. and J. C. Larue. 1990. The decay power law in grid-generated turbulence. J. Fluid Mech., *219,* 195–214.

Nokes, R. I. 1988. On the entrainment rate across a density interface. J. Fluid Mech., *188,* 185–204.

Osborn, T. R., D. M. Farmer, S. Vagle, S. A. Thorpe, and M. Cure. 1992. Measurements of bubble plumes and turbulence from a submarine. Atmos. Ocean, *30,* 419–440.

Price, J. F. 1979. On the scaling of stress driven entrainment experiments. J. Fluid Mech., *90,* 509–529.

Rodi, W. 1987. Examples of calculation methods for flow and mixing in stratified fluids. J. Geophys. Res., *92,* (C5), 5305–5328.

Rohr, J. J., E. C. Itsweire, K. N. Helland and C. W. van Atta. 1988. Growth and decay of turbulence in a stably stratified shear flow. J. Fluid Mech., *195,* 77–111.

Shih, L. H., J. R. Koseff, J. H. Ferziger and C. R. Rehmann. 2000. Scaling and parameterization of stratified homogeneous turbulent shear flow. J. Fluid Mech., *412,* 1–20.

Speziale, C. G., R. Abid and E. C. Anderson. 1990. A critical evaluation of two-equation models for near-wall turbulence. AIAA paper 90-1481, AIAA, Seattle, WA, USA, 1990.

Tavoularis, S. and S. Corrsin. 1981a. Experiments in a nearly homogenous turbulent shear flow with a uniform mean temperature gradient. Part 1. J. Fluid Mech., *104,* 311–348.

———— 1981b. Experiments in a nearly homogenous turbulent shear flow with a uniform mean temperature gradient. Part 2. The fine structure. J. Fluid Mech., *104,* 349–367.

Tavoularis, S. and U. Karnik. 1989. Further experiments on the evolution of turbulent stresses and scales in uniformly sheared turbulence. J. Fluid Mech., *204,* 457–478.

Tennekes, H. 1989. The decay of turbulence in plane homogeneous shear flow, *in* Lecture Notes on Turbulence, J. R. Herring and J. C. McWilliams, eds., World Scientific, 32–35.

Terray, E. A., M. A. Donelan, Y. C. Agrawal, W. M. Drennan, K. K. Kahma, A. J. Williams III, P. A. Hwang and S. A. Kitaigorodskii. 1996. Estimates of kinetic energy dissipation under breaking waves. J. Phys. Oceanogr., *26,* 792–807.

Terray, E. A., W. M. Drennan and M. A. Donelan. 1999. The vertical structure of shear and dissipation in the ocean surface layer, *in* The Wind-Driven Air-Sea Interface. Electromagnetic and Acoustic Sensing, Wave Dynamics and Turbulent Fluxes, M. L. Banner, ed., School of Mathematics, University of NSW, Australia, 239–245.

Thompson, S. M. and J. S. Turner. 1975. Mixing across an interface due to turbulence generated by an oscillating grid. J. Fluid Mech., *67,* 349–368.

Thorpe, S. A. 1984. On the determination of K_v in the near-surface ocean from acoustic measurements of bubbles. J. Phys. Oceanogr., *14,* 855–863.

Thorpe, S. A., T. R. Osborn, J. F. E. Jackson, A. J. Hall, and R. G. Lueck. 2003. Measurements of turbulence in the upper-ocean mixing layer using Autosub. J. Phys. Oceanogr., *33,* 122–145.

Townsend, A. A. 1976. The Structure of Turbulent Shear Flow, Cambridge University Press, 444 pp.

Umlauf, L., H. Burchard and K. Hutter. 2003. Extending the k-ω turbulence model towards oceanic applications. Ocean Model., *5,* 195–218.

Wilcox, D. C. 1988. Reassessment of the scale-determining equation for advanced turbulence models. AIAA Journal, *26,* 1299–1310.

———— 1998. Turbulence Modeling for CFD. DCW Industries, Inc., 2nd edition, 1998.

Zeierman, S. and M. Wolfshtein. 1986. Turbulent time scale for turbulent-flow calculations. AIAA J., *24,* 1606–1610.